Published in: Colloids and surfaces B: biointerfaces (2000), vol. B19, iss. 4, pp. 381-395
Status: Postprint (Author's version)

Microphase separation at the surface of block copolymers, as studied with atomic force microscopy

A. Rasmont [(1)], Ph. Leclère [(1)], C. Doneux [(1)], G. Lambin [(1)], J.D. Tong [(2)], R. Jérôme [(2)], J.L. Brédas [(1)], R. Lazzaroni [(1)]

[(1)] Service de Chimie des Matériaux Nouveaux, Centre de Recherche en Electronique et Photonique Moleculaires,
Universite de Mons-Hainaut, Place du Parc 20, B-7000 Mons, Belgium
[(2)] Centre d'Etude et de Recherche sur les Macromolecules (CERM), Université de Liège, Sart-Tilman B6, B-4000 Liège, Belgium

Abstract

Atomic force microscopy (AFM) is used to study the phase separation process occurring in block copolymers in the solid state. The simultaneous measurement of the amplitude and the phase of the oscillating cantilever in the tapping mode operation provides the surface topography along with the cartography of the microdomains of different mechanical properties. This technique thus allows to characterize the size and shape of those microdomains and their organization at the surface (e.g. cubic lattice spheres, hexagonal lattice of cylinders, or lamellae). In this study, a series of symmetric triblock copolymers made of a inner elastomeric sequence (poly(butadiene) or poly(alkylacrylate)) and two outer thermoplastic sequences (poly(methylmethacrylate)) is analyzed by AFM in the tapping mode. The microphase separation and their morphology are essential factors for the potential of these materials as a new class of thermoplastic elastomers. Special attention is paid to the control of the surface morphology, as observed by AFM, by the molecular structure of the copolymers (volume ratio of the sequences, molecular weight, length of the alkyl side group) and the experimental conditions used for the sample preparation. The molecular structure of the chains is completely controlled by the synthesis, which relies on the sequential living anionic polymerization of the comonomers. The copolymers are analyzed as solvent-cast films, whose characteristics depend on the solvent used and the annealing conditions. The surface arrangement of the phase-separated elastomeric and thermoplastic microdomains observed on the AFM phase images is discussed on the basis of quantitative information provided by the statistical analysis by Fourier transform and grain size distribution calculations.

Keywords: Block copolymer; Atomic force microscopy; Phase separation; Surface segregation

1. Introduction

Over the past few years, self-organization on the nanometer scale has become a major topic of research in materials science. Novel approaches have recently appeared for the controlled synthesis and assembly of metal and semiconductor nanoparticles [1]. In practice, these materials are prepared as colloids consisting of well-defined nanocrystals coated by a sheath of short organic chains that prevent aggregation. Independently of numerous potential applications, such metal nanocrystals and semiconductor quantum dots are ideal candidates to study quantum effects on the charge transport properties and linear and non-linear optical response. Where the organic materials and polymers are concerned, a much wider range of nanoscale objects of controlled size and shape can be produced, going from the formation of micelles to the dewetting of thin films or to the design, synthesis, and assembly of complex supramolecular structures such as dendrimers and block copolymers.
The development of new analytic techniques has greatly contributed to the progress study of nanoscale materials, be they inorganic or organic. Among other techniques, the advent of scanning probe microscopies (scanning tunneling microscopy (STM) and atomic force microscopy (AFM)) has improved the direct observation of structures and assemblies [2,3]. These techniques provide structural information in direct space with unprecedented lateral and vertical resolution. Since AFM does not require the samples to be electrically conductive, this technique is best suited to the investigations of organic compounds, most of which are insulating. Because the tip is in physical contact with the sample, the AFM apparatus can be employed as a local probe to map the surface properties, such as friction and elastic modulus, or to estimate the strength of interface interactions [4] and covalent bonds [5,6].
In this work, Tapping-Mode AFM (TMAFM) [7] is used in order to improve the understanding of the

supramolecular organization at the surface of thin films of block copolymers. Because most polymers are non-miscible, the constitutive components of block copolymers tend to phase separate into chemically homogeneous domains. However, the covalent bonds of these components prevents phase separation from extending over a large length scale. Instead, only small domains with typical sizes in the range of tens of nanometers are formed. The dependence of bulk morphology on the composition of diblock copolymers has been analyzed experimentally by scattering techniques and transmission electron microscopy and is now well understood [8–15]. For instance, copolymers of symmetric composition (i.e. around 50% in each constituent), arrange themselves as an alternating array of lamellae parallel to each other.

The microdomain organization at the surface of block copolymers is a very important issue because the chemical nature of the surface governs its interactions with the surrounding medium and thus with other materials. Compared with the bulk, the morphology at the surface is expected to be strongly affected by the interface with air. Surface segregation phenomena in block copolymers have been intensively studied over the past 2 decades, mainly by surface-sensitive spectroscopies [16,17] and more recently by scanning probe techniques [18–20].

This paper reports on a systematic AFM study of a series of symmetric triblock copolymers, with molecular structures typical of thermoplastic elastomers (TPE's). The central block of these triblocks consists of a rubbery polymer (i.e. the glass transition temperature (T_g) lower than room temperature) which is the major component of the copolymer. The outer two blocks are short length thermoplastics (i.e. T_g well above the ambient temperature). Below T_g, the thermoplastic microdomains are rigid and act as physical crosslinks for the elastomeric matrix, such that the triblock behaves as a vulcanized rubber. Above the T_g of thermoplastic microdomains the copolymer flows and the material can be processed by traditional techniques. TPE's are therefore spontaneously and thermoreversibly crosslinked rubbers.

The chemical structure of these triblock copolymers discussed here is shown in Scheme 1. Two identical thermoplastic sequences of poly(methyl-methacrylate), PMMA, are attached to a central sequence of poly(butadiene) and low T_g poly(alkylacrylate). These compounds will be designated as MBM and MAM, respectively. Compared with classical TPE's based on styrene–butadiene–styrene copolymers, these copolymers herein show broader service temperature range (because T_g of PMMA is higher than T_g of polystyrene). Resistance to oxidation is also improved when poly(alkylacrylate) in MAM is used rather than poly(butadiene) in MBM.

Very importantly, the properties typical of TPE are observed when: (i) all the triblock chains are of low size and composition dispersity which can be achieved by controlled or living copolymerization [21,22]; and (ii) the microphase separation is sharp. Formation of the phase-separated microdomains and their assembly on the surface have been studied in relation to the macroscopic mechanical and rheological properties measured independently [23]. The AFM analysis consists in recording both the amplitude and the phase of the oscillating tip as it scans the sample surface. Whereas the amplitude data provide topographic information, the phase data (i.e. the phase difference between the periodic signal exciting the cantilever and the response at the photodiode array that detects the cantilever movements) are very sensitive to the interaction between the tip and the surface. This characteristic allows areas of different chemical composition to be distinguished. This operation mode is often called 'phase detection imaging' (PDI).

This paper is structured as follows. After a brief description of the samples preparation and imaging, we discuss the influence of the composition of TPE's on their morphology. We then illustrate how morphological transitions can take place at the surface, as a function of the preparation conditions of the copolymer films.

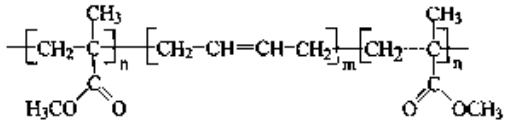

MBM

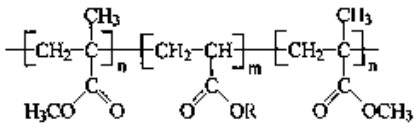

R = ethyl, propyl, *n*-butyl, *i*-octyl

MAM

Scheme 1.

Attention is paid to the influence of the solvent used to cast the films, the solvent evaporation rate, and the thermal annealing above T_g of the thermoplastic component. Finally, the influence of the molecular structure, particularly the size of the alkyl group of the central poly(alkylacrylate) block in MAM on the microphase separation is discussed.

2. Experimental section

2.1. Synthesis of triblock copolymers

All the triblock copolymers were synthesized by classical anionic polymerization. For the MBM series, the procedure was based on a difunctional anionic initiator ($DIBLi_2$) prepared by addition of *t*-butyllithium (*t*-BuLi) to 1,3-diisopropenylbenzene (DIB), as described elsewhere [24–32].
For the MAM copolymers, the first step in the synthesis consisted in preparing a triblock copolymer with a central sequence of poly(*t*-butylacrylate). This precursor triblock was then converted into the desired MAM by transalcoholysis of the *t*-butyl ester groups [23].

2.2. Sample preparation and AFM imaging

Thin copolymer films were cast on freshly cleaved muscovite mica substrates from dilute solutions in THF or toluene (2 mg ml^{-1}). The solvent was evaporated very slowly for 1 day at room temperature either in air or in a solvent-saturated atmosphere. The final film thickness was ca. 500 nm, as determined by profilometry. The films were observed by AFM as such or after annealing at 140°C under high vacuum for 24 h. They remain colorless with a smooth surface.
All the AFM images were recorded with a Nanoscope IIIa microscope from Digital Instruments Inc. in the tapping mode (25°C, in air). Microfabricated silicon cantilevers were used with a spring constant of 30 Nm^{-1}. The instrument was equipped with the Extender™ Electronics Module to provide simultaneously height and phase cartography. Images of different areas of each sample were recorded, and the scanning time was ca. 5 min. The images were recorded in the so-called 'soft tapping mode', to avoid deformation and indentation of the polymer surface by the tip.

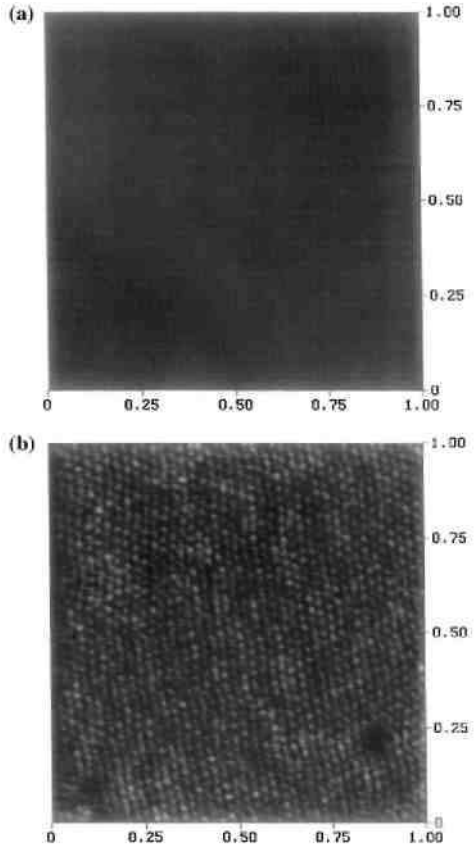

Fig. 1. TMAFM height (a) and phase (b) images (1 x 1 μm^2) of a PMMA-b-poly(i-octylacrylate)-b-PMMA copolymer (sample MAM-1, Table 1). The grayscale of the height image is 10 nm while the phase image shows

the morphology of the copolymer.

Practically, the A_{sp}/A_0 value was set to 0.95, where A_0 is the free oscillation amplitude and A_{sp} is the setpoint amplitude selected for the measurement. All the images were collected with the maximum available number of pixels (512) in each direction. The Nanoscope image processing software was used for image analysis.

3. Results and discussion

3.1. Microphase separation as observed with phase detection imaging

Fig. 1 shows typical AFM images for the PMMA-*b*-poly(*i*-octylacrylate)-*b*-PMMA triblock containing 12.2 wt% PMMA (corresponding to MAM-1 in Table 1). The height image (Fig. 1a) is very uniform, thus indicating that the surface of the analyzed sample is very smooth (the typical value of the root mean square roughness for a 1 x 1 μm^2 area is 1.4 nm). This observation guarantees that the contrast observed in the PDI image does not originate from differences in surface topography. The phase image (Fig. 1b) clearly shows a two-phase morphology, which consists of an assembly of bright round-shaped objects in a darker matrix. These objects appear arranged in a regular pattern. Based on what it is known about the morphology of block copolymers [33] in this composition range, the AFM phase image can readily be interpreted as spheres of PMMA in a poly(*i*-octylacrylate), PIOA, matrix.
However, it must be stressed that the AFM phase images can be interpreted without the *a priori* knowledge of the phase morphology, provided that a relationship, at least qualitative, between the phase shift and the properties of the probed material is available.

Table 1
Molecular characteristics of the MAM triblock copolymers considered in this study

Sample	Alkyl group	Molecular weight (M_n ($\times 10^{-3}$))	M_w/M_n	% PMMA
MAM-1	*i*-Octyl	7–100-7	1.07	12.2
MAM-2	*i*-Octyl	20–140–20	1.04	22.2
MAM-3	*i*-Octyl	40–140–40	1.06	36.4
MAM-4	*n*-Butyl	30–150–30	1.05	28.6
MAM-5	*n*-Butyl	10–50–10	1.06	28.6
MAM-6	Ethyl	10–50–10	1.09	28.6

Over the last couple of years, the origin of the phase contrast in TMAFM has been actively investigated [34,35]. It has been shown that the contrast is related to the local dissipation of the energy brought to the surface by the oscillating tip [36]. It thus strongly depends on the details of the tip–sample interactions; actually these interactions depend not only on the intrinsic properties of the analyzed material, particularly its elastic and viscoelastic moduli, but also on the mechanical properties of the tip and the tip–sample adhesion. The quantitative measurement of the mechanical properties of the polymer on the local scale from PDI-TMAFM data is therefore a very delicate task. Nevertheless, the qualitative interpretation of the PDI images in reference to the spatial distribution of domains of a heterogeneous surface is possible. Indeed, the magnitude of the phase shift is known to be directly related to the elastic modulus of the sample in the 'soft tapping' regime used in this study, i.e. when the amplitude of the oscillating cantilever is only slightly reduced (for instance, for A_{sp}/A_0=0.95) by interaction with the surface [37,38]. Recently, a quantitative approach based on the analytical expressions derived from the non-linear behavior of an oscillating tip– cantilever system was proposed [39–42]. This theoretical model can fit to different situations in the tapping mode (non-contact as well as intermittent contact). By fitting the approach–retract curves, it is possible to distinguish the different domains in terms of elastic moduli [43]. In the present case, a factor of 3 has been found between the modulus of the harder domains (PMMA) and the modulus of the softer domains (poly(*i*-octylacrylate), PIOA). According to the approaches in Refs. [37–42], the bright spots in Fig. 1(b) can be assigned to spheres of PMMA (the harder component leading to a larger phase shift) while the darker matrix is made of the softer component (PIOA). The PDI-TMAFM images of block copolymers should be carefully analyzed along two lines: (i) since the imaging of the phase lag cannot be directly compared (throughout this paper, the grayscale of the PDI images has been chosen to make visualization easier); (ii) the morphology can be drastically modified when the film thickness is of the same order of magnitude as the phase-separated domains, typically a few tens of nanometers [44]. In such a case, the interactions of the different blocks with the substrate can favor specific assemblies. This aspect has not been considered in this study, since deposits with a thickness (= 500 mm) at least ten times as large as the domain size have been prepared; so, the observed morphology should be independent of the nature of the substrate, but

typical of the polymer/air interface. The validity of this feature has been confirmed by the analysis of a number of 1 mm-thick, free-standing samples; whose the surface morphology proved to be essentially the same as the 500-nm parent films, even though some topographic features can be perturbed by higher surface roughness.

3.2. Influence of the composition

The equilibrium phase morphology of block copolymers depends on the copolymer composition. This relationship has been intensively investigated experimentally and rationalized theoretically for styrene-isoprene block copolymers [45-47]. A spherical morphology is observed for polystyrene (PS) contents lower than 20 vol%; or contents between 20 and 35 vol%, hexagonal arrangement of PS cylinders is observed, whereas a lamellar morphology is reported in the 40-65 vol% range. Finally, for compositions richer in PS, cylindrical and spherical assemblies of poly-isoprene are found, as expected. It is also worth noting that a bicontinuous gyroïd morphology has been discovered for compositions intermediate between those leading to cylinders and lamellae [48-50].

3.2.1. PMMA -b -poly(alkylacrylate)-b -PMMA copolymers

Fig. 2 shows the phase images observed for the three PMMA-*b*-poly(*i*-octylacrylate)-*b*-PMMA copolymers listed in Table 1 (samples MAM-1, MAM-2, and MAM-3). For the lowest PMMA content (~ 12%), the film surface clearly consists of an assembly of bright PMMA spheres in a dark PIOA matrix (Fig. 2a). These spheres appear to be arranged in a hexagonal lattice, as indicated by the two-dimensional Fourier transform of the image shown as inset.

This surface morphology is thought to correspond to a particular face of the body-centered cubic lattice expected in this composition range. Image analysis indicates that the average distance between sphere centers is about 27 nm. Increasing the PMMA content above 20% (MAM-2, Table 1) leads to a morphological transition (Fig. 2b). Bright elongated objects appear in a darker continuous matrix; they are believed to originate in PMMA cylinders (bright areas) lying parallel to the surface, within the poly(*i*-octylacrylate) matrix. The width of the flat cylinders is about (19 ± 1) nm. The phase image for sample MAM-3 (Table 1) is highly textured (Fig. 2c), consisting of a complex pattern of bright and dark elongated objects. This pattern is interpreted as an interpenetrated assembly of PMMA and PIOA lamellae, which is consistent with the copolymer composition range. As discussed above, the brighter areas correspond to larger phase values and are typical of the component of higher modulus, i.e. PMMA; the darker areas are the signature of the softer component, poly(*i*-octylacrylate) in this case. We stress that the phase image is not reminiscent at all of the topographic profile. It is fully dominated by the local contrast in mechanical properties, thus providing clear evidence for microphase separation in such a triblock copolymer. Besides these three examples, that illustrates the three major morphologies, a systematic AFM analysis of a larger series of PMMA-*b*-PIOA-*b*-PMMA (MIM) compositions has been conducted, and in all cases, a microdomain morphology consistent with the expectations based on the copolymer composition has been observed [33].

Published in: Colloids and surfaces B: biointerfaces (2000), vol. B19, iss. 4, pp. 381-395
Status: Postprint (Author's version)

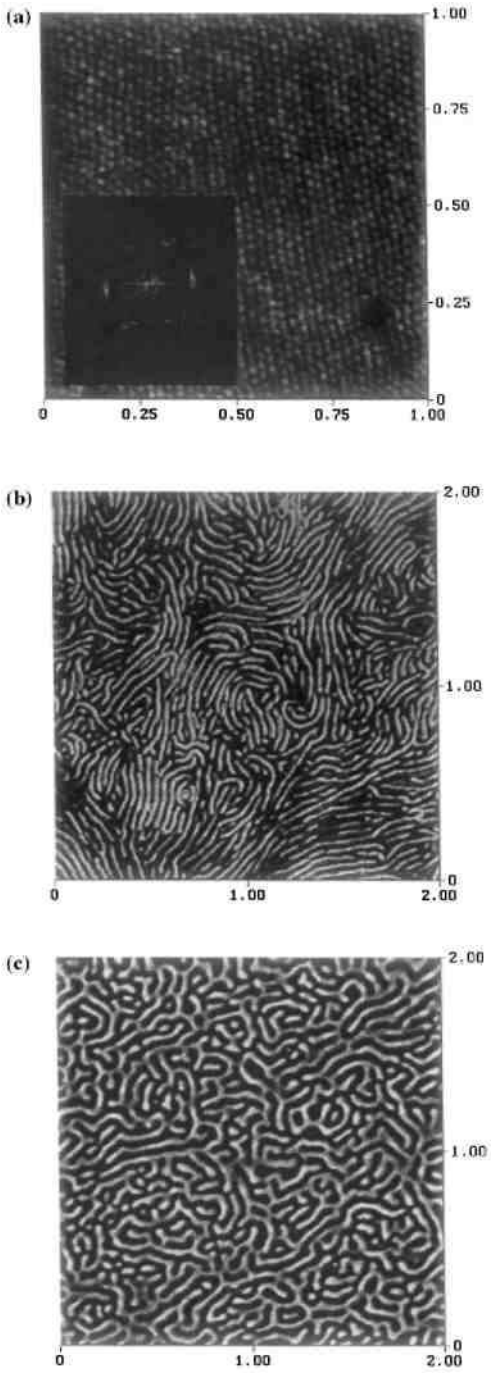

Fig. 2. TMAFM phase images of the PMMA-b-poly(i-octylacrylate)-b-PMMA triblock copolymers listed in Table 1: (a) spherical morphology (sample MAM-1); (b) cylindrical morphology (sample MAM-2); (c) lamellar morphology (sample MAM-3). The inset shows that the PMMA domains are arranged in a hexagonal lattice.

3.2.2. PMMA -b -poly(butadiene)-b -PMMA copolymers

The same approach has been used for the analysis of additional series of thermoplastic elastomers, e.g. the PMMA-*b*-poly(butadiene)-*b*-PMMA (MBM) copolymers (samples MBM-1 to MBM-4 in Table 2) [24-32]. Fig. 3(a-c) show the phase images for three MBM triblock copolymers containing 12.5, 33, and 50% PMMA, respectively. The evolution is very similar to that we described above. Fig. 3(a) is a dispersion of PMMA spheres in a poly(butadiene) (PBD) matrix, which however appears less ordered than in the corresponding MIM copolymers. Fig. 3(b) shows an assembly of short, bright cylinders.

Published in: Colloids and surfaces B: biointerfaces (2000), vol. B19, iss. 4, pp. 381-395
Status: Postprint (Author's version)

Table 2
Molecular characteristics of the MBM triblock copolymers considered in this study

Sample	Molecular weight (M_n ($\times 10^{-3}$))	M_w/M_n	% PMMA
MBM-1	6–85–6	1.10	12.4
MBM-2	16–65–16	1.10	33.0
MBM-3	50–100–50	1.15	50.0
MBM-4	20–36–20	1.12	52.6

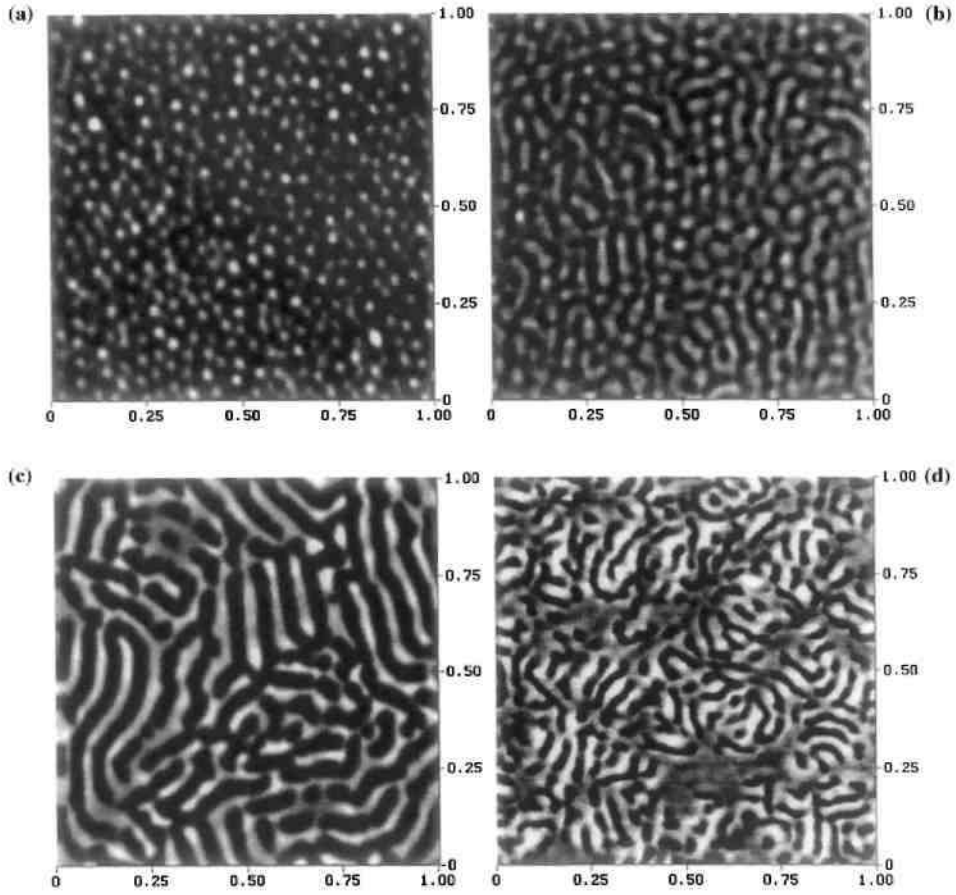

Fig. 3. TMAFM phase images of the PMMA-b-poly(butadiene)-b-PMMA triblock copolymers listed in Table 2: (a) spherical morphology (sample MBM-1); (b) cylindrical morphology (sample MBM-2); (c) and (d) lamellar morphology in sample MBM-3 and sample MBM-4, respectively.

For a composition close to 50:50, a lamellar morphology is observed, as expected (Fig. 3c and d).
Note that the typical width of the lamellae observed in Fig. 3(c and d) is markedly different in the samples MBM-3 and MBM-4, despite a very similar the copolymer composition (see Table 2). A Fourier transform analysis indicates that the spatial period typical of sample MBM-3 is 63 versus 47 nm in sample MBM-4. This difference results from the variation in molecular weight between the two copolymers. It has been shown that the periodicity of the microdomain depends on the molecular weight according to a power-law [51].
Even though the analysis of only two compositions does not allow the power-law dependence to be checked accurately, the observed evolution in the domain size is qualitatively consistent with the behavior.

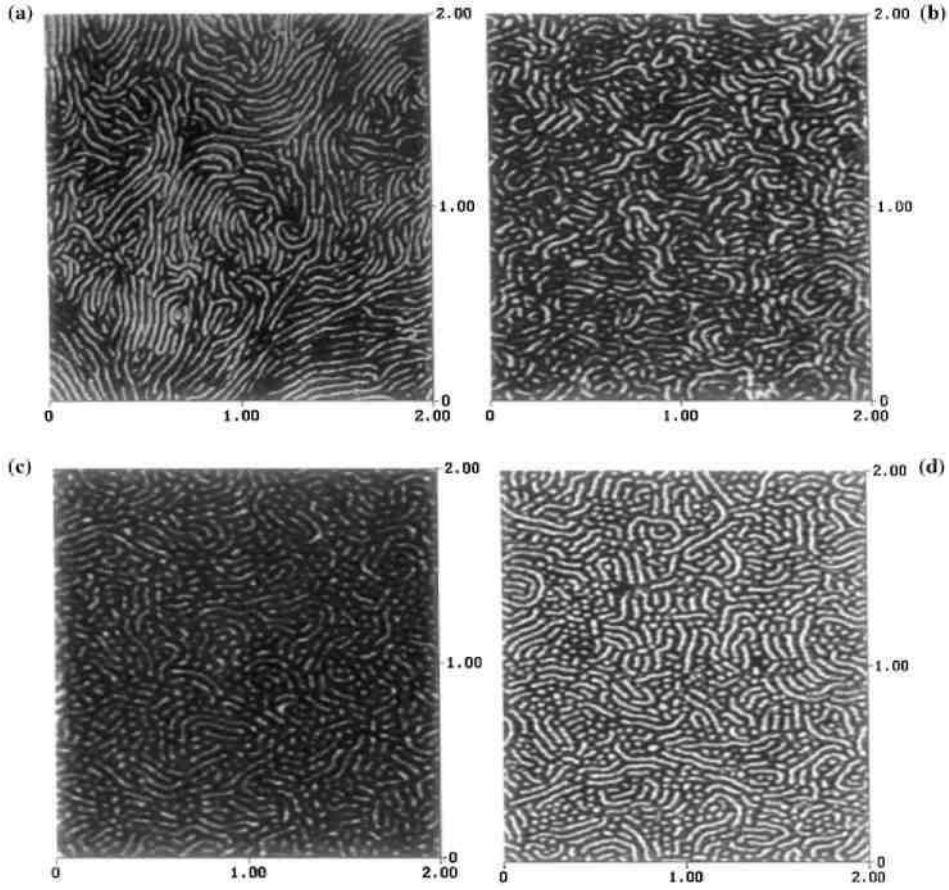

Fig. 4. TMAFM phase images of a selected PMMA-b-poly(i-octylacrylate)-b-PMMA triblock copolymer (sample MAM-2, Table 1): film prepared from THF and (a) dried in air; (b) dried in THF-saturated atmosphere; film prepared from toluene and (c) dried in air; (d) dried in toluene-saturated atmosphere.

3.3. Influence of the sample preparation

3.3.1. Influence of solvent

The solvent used to prepare the copolymer films can exert a strong influence on the morphology, mainly because the solubility of the constitutive blocks can be different, which leads to selective precipitation during the casting process. Two solvents has been compared in this study, THF and toluene, which are good solvents for both the thermoplastic blocks (PMMA) and the elastomer poly(*i*-octylacrylate). For sample MAM-2, the surface morphology has been compared for films prepared from the two solvents and dried either in open air or in a solvent-saturated atmosphere. Typically, the samples were dried at room temperature for 48 h. However, samples prepared from the more volatile solvent (THF) and dried in air were available in a few minutes. The AFM images are collected in Fig. 4.

The films prepared in THF and dried in air (Fig. 4a) show the cylindrical morphology already described above. When the films are prepared from a THF-saturated atmosphere or from toluene, the surface shows a more complex morphology (Fig. 4b–d): the cylinders tend to be shorter and a number of bright round-shaped objects are also observed on the surface. These objects are believed to be PMMA cylinders standing perpendicular to the surface, in such a way that only their apex is visible.

For the purpose of a more quantitative analysis a grain-size analysis of the images shown in Fig. 4 has been performed. This analysis consists in establishing the distribution of the bright objects according to their size. The corresponding histograms reflect the grain-size distribution. Each class corresponds to the average surface of the domains and the number within the class is the number of domains. A 'domain' is defined in terms of scan lines of a known minimum and maximum size above a certain user-defined threshold.

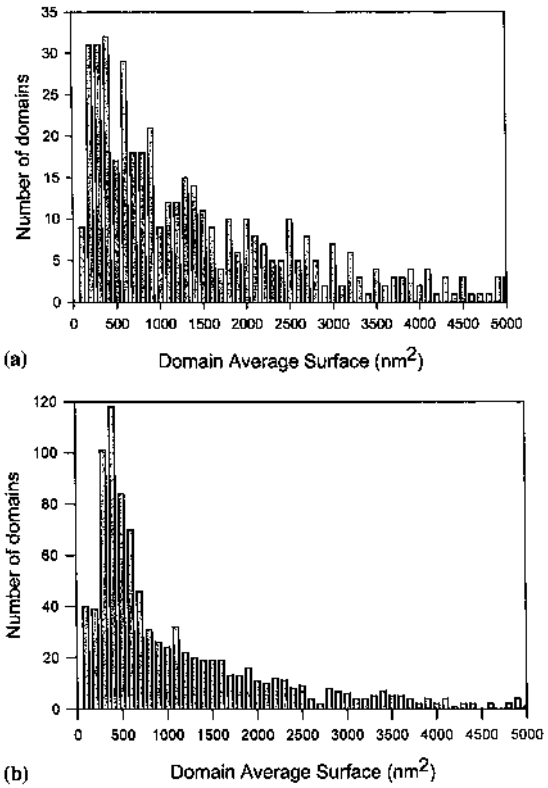

Fig. 5. Distribution of the size of the PMMA microdomains for the images of (a) Fig. 4(a), and (b) Fig. 4(d).

When attention is paid to the round-shaped objects assumed to be cylinders perpendicular to the surface, their contribution to the total area of the bright domains is negligible (- 1%) in Fig. 4(a); then it increases to 22% in Fig. 4(b), to 39% in Fig. 4(c), finally reaching 53% in Fig. 4(d). This evolution is illustrated for two images by the grain size distributions shown in Fig. 5. The image in Fig. 4(a) is characterized by a distribution decreasing gradually towards the larger areas. Note that Fig. 5(a) is the 'unweighted' number distribution; the area-weighted distribution (not shown here), emphasizing the predominant contribution of the large-area domains. In contrast, the domain size distribution computed from Fig. 4(d) shows a well-defined peak around 400 nm^2 (Fig. 5b), as result of the large number of small, round-shaped objects. This observation clearly shows that the solvent used to cast the film and the evaporation rate strongly influence the surface morphology: fast evaporation of THF leads to cylinders lying flat on the surface (Fig. 4a) whereas the cylinders tend to arrange perpendicular to the surface upon slow evaporation of toluene (Fig. 4d). The cylinder orientation is interpreted on the basis of thermodynamic arguments below. Beyond the effect of the evaporation rate, the interplay of the solvent/polymer/air interactions more likely has an effect on the surface morphology.

3.3.2. Influence of annealing conditions

The morphology of block copolymers is also expected to depend on the thermal annealing. When the sample is annealed at above the glass transition temperature of the two blocks, the increase in chain mobility allows the morphology to change. Fig. 6 shows images of the same film (sample MAM-2, Table 1) before Fig. 6(a) and after Fig. 6(b) annealing at 140°C for 24 h. It must be noted that longer annealing times have no effect on the morphology, which suggests that the thermodynamic equilibrium has been reached after 24 h. Before annealing, the surface is a combination of PMMA cylinders, lying flat and perpendicular to the surface; the width of the flat cylinders (30 ± 2 nm) being identical to the diameter of the cylinders standing upright.
The annealing thus influences strongly the morphology, since almost all the cylinders perpendicular to the surface amount to 93% of the total area of the PMMA domains after annealing compared with 53% before annealing.

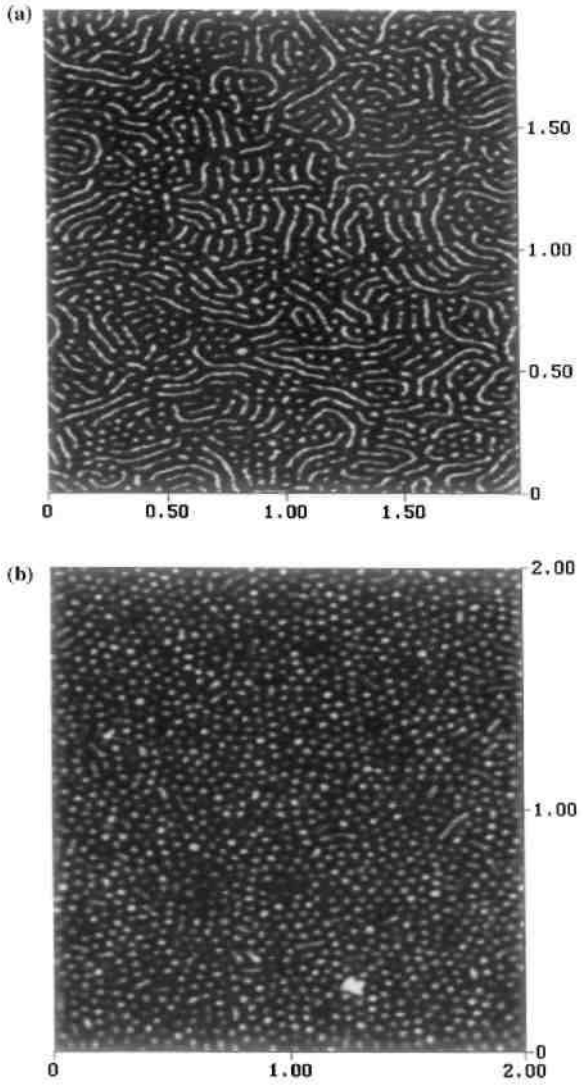

Fig. 6. TMAFM phase images of the PMMA-b-poly(i-octylacrylate)-b-PMMA triblock copolymer listed sample MAM-2 in Table 1, prepared from toluene solution evaporated in a toluene-saturated atmosphere (a) before and (b) after annealing at 140°C for 24 h.

3.3.3. Interpretation of the morphology

In order to account for the dependence of the surface morphology of the MBM and MAM copolymers, both the solvent and the annealing process can modify the surface morphology of these triblock copolymers. The observed morphologies can be understood on the basis of an enthalpy/entropy compromise. Fig. 7 compares three morphologies for the same triblock copolymer (MAM-2, Table 1), i.e. (a) cylinders lying flat on the surface; (b) a combination of flat and standing-up cylinders; and (c) mostly standing-up cylinders, respectively. These observations show that the ratio between standing and flat cylinders tends to increase upon slow evaporation and/or upon annealing; this suggests that the most stable arrangement for the PMMA cylinders is perpendicular to the surface (Fig. 8). This is consistent with the higher surface energy of PMMA (42.7 mJ cm^{-2}) compared with poly(i-octylacrylate) (34.3 mJ cm^{-2}) [52]. This triggers the system to organize itself so as to minimize the amount of PMMA at the surface, thus by exposing only the apex of the PMMA cylinders. In Fig. 7(b), it is likely that the sample is not reached full thermodynamic equilibrium, since flat cylinders remain visible on the surface; whereas almost all cylinders are standing-up in Fig. 7(c), only a few short segments lying flat on the surface.
This evolution is fully consistent with the corresponding domain size distributions shown in Fig. 9. The surface distribution is very broad for the sample solvent-cast in air and before annealing (Figs. 7a and 9a). Only 1% of the total area of the PMMA domains of Fig. 7(a) corresponds to standing-up cylinders, while this proportion jumps to 41 and 72% for the domains of Fig. 7(b and c), respectively. The average surface occupied by the PMMA domains over the whole Fig. 7(c) is ca. 400 nm^2, which corresponds to cylinders with a diameter of 23

nm. The distribution typical of the 'mixed' morphology (Figs. 7b and 9b) shows a broad peak centered around 700 nm^2; this peak contains the distribution of the standing-up cylinders and the large number of short flat cylinders, which can be viewed as 'bridges' between two cylinders developing downwards perpendicular to the surface. As a result, the size distribution is shifted towards larger areas (Figs. 7b and 9b), compared with the situation where all the standing-up cylinders are present (Figs. 7c and 9c).

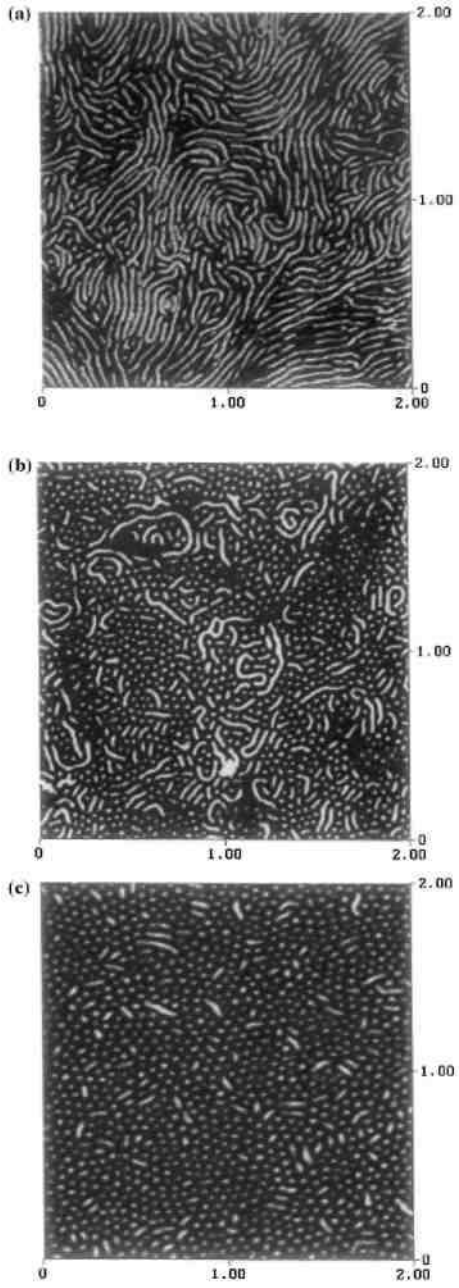

Fig. 7. TMAFM phase images of the PMMA-b-poly(i-octylacrylate)-b-PMMA triblock copolymer listed sample MAM-2 in Table 1, prepared from a THF solution (a) in air, non-annealed; (b) in air, annealed; (c) in a THF-saturated atmosphere, annealed.

This 'mixed' morphology could result from the interplay of entropic (i.e. surface disordering) and enthalpic (i.e. surface energy) factors. A reasonable explanation might be that the entropic gain which results from the disordered assembly of cylinders is partly overcome by the enthalpic loss of bringing more PMMA to the surface, even at moderate temperatures. It must be noted that mixed arrangements of cylinders have been observed previously, in very thin layers of styrene– butadiene–styrene copolymers [53,54].
As expected, when the PMMA content of the block copolymers is increased up to ca. 50%, a lamellar morphology is observed as illustrated in Figs. 2(c) and 3(c and d). The alternation of dark and bright stripes

originates from the lamellae of the soft and hard components, assembled perpendicular to the surface. The orientation of the lamellae in thin films of block copolymers has received considerable attention in the recent years [55,56]. It has been shown that, under near equilibrium conditions, the lamellae formed by diblock copolymers are preferably oriented parallel to the surface, with the lamellae lying on top of each other parallel to the substrate. Actually, the film is organized in such a way that the component with the smaller surface energy forms the outer lamella (this situation is sketched in Fig. 10a). It has also been shown that this preferential orientation occurs at both the air/copolymer and copolymer/substrate interfaces and that the surface-induced orientation in solution-cast films is independent of the film thickness [57]. Therefore, under near equilibrium conditions, perpendicular lamellar structures are usually not observed at the surface of diblock copolymers. Exceptions to this situation can occur when confining the films between two rigid surfaces [58] (in which case, if there is no preferential adsorption lamellae can be oriented perpendicular to the interfaces) or when the film thickness is exactly one lamellar repeat spacing [59] (as soon as the thickness is larger than one lamellar period, the lowest energy structure in diblock copolymer is one with lamellae oriented parallel to the free surface (polymer/air interface) of the film).

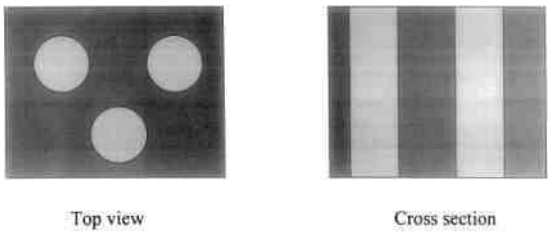

Fig. 8. Schematic representation of a cylindrical arrangement of block copolymers. The light gray and dark gray areas correspond to the component with the highest and the lowest surface energy, respectively: (a) top view; (b) cross section. In this scheme, the cylinders are standing-up perpendicular to the surface.

In the case of the MBM and MAM triblock copolymers discussed here, the same arrangement, thus with the less polar central block exposed to the surface should force all the chains to present loops and the external PMMA blocks to be buried in a lamella beneath the surface (Fig. 10b). Since this type of organization is expected to result in a significant loss in conformational entropy, an arrangement of lamellae perpendicular to the surface (Fig. 10c), with the central block extended or looped would be thermodynamically more favorable. Since the difference in surface energy between the components is rather small, the gain in entropy can overcome the energetic penalty due to the localization of the most polar component at the surface. Therefore, this unusual lamellar organization is the direct consequence of the molecular architecture of the triblock copolymers and not of the sample thickness or the interactions with the substrate. To our best knowledge, this is the first example of the spontaneous orientation of lamellae perpendicular to the surface of in two-component block copolymers.

3.4. Influence of the alkyl group in the central Poly(acrylate) block

We now turn to a discussion of the effect of the length of the alkyl group in the acrylate units of the central block. The surface morphology of triblock copolymers of comparable PMMA contents but containing different alkylacrylate in the central block, i.e. *n*-butyl, *n*-propyl and ethyl, has
been obtained. Fig. 11(a) corresponds to the 30 000–150 000–30 000 copolymer (sample MAM-4, Table 1). PMMA cylinders (bright areas), either standing perpendicular or lying parallel to the surface, within the poly(*n*-butylacrylate) matrix (Fig. 11a).

Published in: Colloids and surfaces B: biointerfaces (2000), vol. B19, iss. 4, pp. 381-395
Status: Postprint (Author's version)

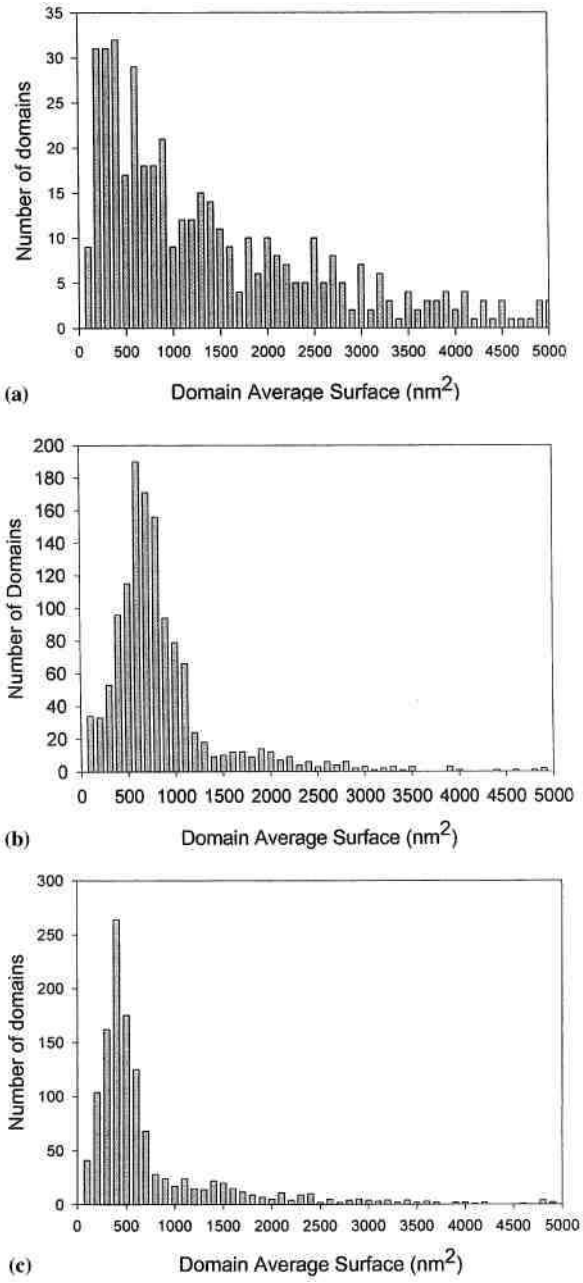

Fig. 9. Histograms of the size of the PMMA microdomains corresponding to the images of Fig. 7.

Published in: Colloids and surfaces B: biointerfaces (2000), vol. B19, iss. 4, pp. 381-395
Status: Postprint (Author's version)

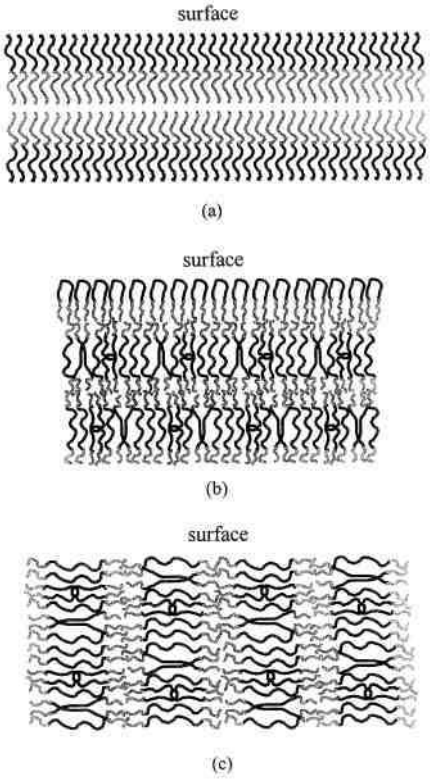

Fig. 10. Schematic representation of lamellar arrangements of block copolymers. The light gray and dark gray sequences correspond to the components with the highest and the lowest surface energy, respectively. The outer surface is the area above each sketch: (a) in a diblock copolymer, lamellae arrange parallel to the surface, exposing only the low-energy component; (b) in a symmetric copolymer with polar outer segments, parallel arrangement of the lamellae implies that all central segments form loops; (c) alternative arrangement of lamellae of the symmetric triblock copolymer, with both components exposed to the surface.

A similar morphology is found in Fig. 11(b) for the 20 000–90 000–20 000 copolymer (sample MAM-5, Table 1). High molecular weight PMMA-*b*-poly(ethylacrylate)-*b*-PMMA copolymers, also microphase separate (not shown here), although the AFM phase image for low molecular weight copolymer (sample MAM-6, Table 1), is completely featureless, indicating the absence of microphase separation (Fig. 11c). This observation more likely results from the combined effect of the similar chemical structure of the blocks and their low molecular weight values.

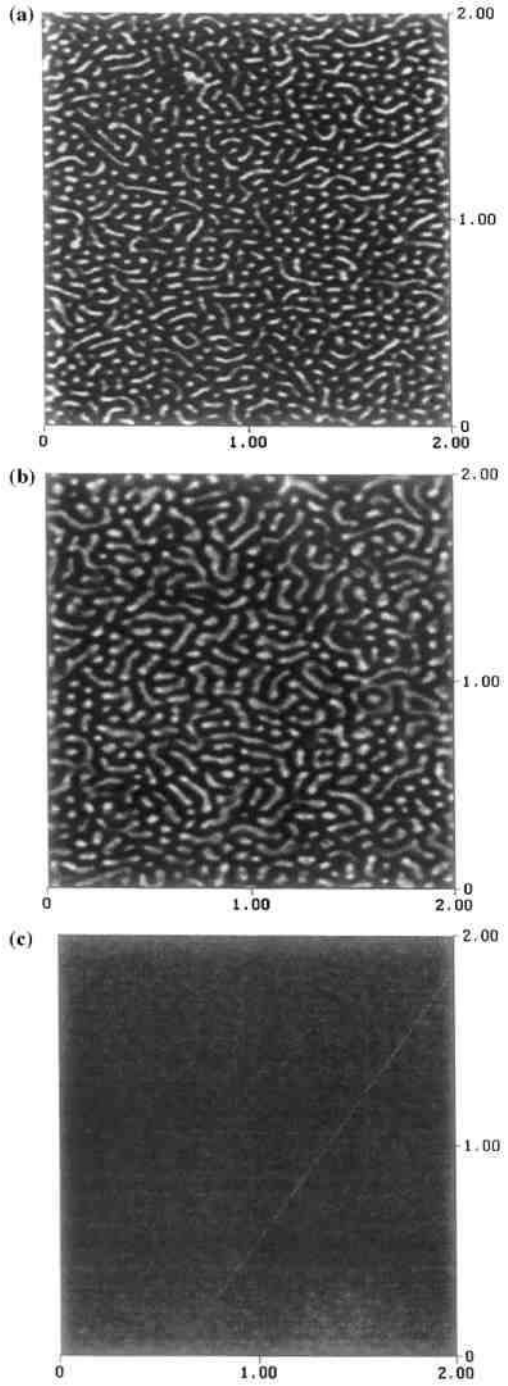

Fig. 11. TMAFM phase images of the PMMA-b-poly(alky-lacrylate)-b-PMMA triblock copolymers with different central poly(alkylacrylate) block (samples MAM-4 to MAM-6, Table 1) (a) n-butyl; (b) n-propyl and (c) ethyl.

For the same reason, no phase separation is observed for th 10 000–50 000–10 000 copolymer, whereas the copolymers all show microphase separation, independently of molecular weight. It is essential to note that the presence or absence of phase separation in this family of materials is fully consistent with the analysis of the mechanical properties reported and discussed elsewhere [23].

4. Conclusions

The phase morphology of poly(methylmethacrylate) - *b* - poly(alkylacrylate) - *b* - poly(methyl -methacrylate) and of poly(methylmethacrylate)-*b*-poly(butadiene)-*b*-poly(methylmethacrylate) triblock copolymers has been studied by atomic force microscopy with phase detection imaging. Spherical, cylindrical, and lamellar morphologies have been observed for block copolymers of increasing PMMA content.

Depending on the experimental conditions for the film casting and annealing, the orientation of the cylinders formed by the minor component with respect to the surface can be modified from a fully parallel organization to a fully perpendicular arrangement. The parallel organization is usually thought to be more thermodynamically stable, since the amount of the most polar component at the surface is then minimized.
In contrast to what happens in diblock copolymers, lamellae formed by symmetric triblock copolymers are always assembled perpendicularly to the surface. We believe that this effect, which is specific for the molecular architecture of the triblock copolymers, could be explained by the folding of the central segment, that is necessary to form a parallel arrangement, leading to an entropic loss which appears to be larger than the enthalpic gain of removing the most polar component from the surface.
Finally, the analysis of a series of triblock copolymers containing different central poly(alkylacrylate) blocks has emphasized the key role of this structural characteristic on the occurrence of the microphase separation, and thus on the performances of the copolymers as thermoplastic elastomers.

Acknowledgements

The collaboration between Mons and Liège is conducted in the framework of the Belgian Federal Government Office of Science Policy (SSTC) *'Pôles d'Attraction Interuniversitaires en Chimie Supramoléculaire et Catalyse Supramoléculaire'* (PAI 4/11). Research in Mons is also partly supported by the European Commission and the Government of the Region Wallonne (Project NOMAPOL-Objectif 1-Hainaut), and the Belgian National Fund for Scientific Research FNRS/ FRFC. AR is holder of a doctoral fellowship of 'Fonds pour la formation a la Recherche dans l'Industrie et dans l'Agriculture' (FRIA). RL is 'Maître de Recherches du Fonds National de la Recherche Scientifique' (FNRS-Belgium).

References

[1] For an overview of recent advances in metal and semiconductor nanostructures, see Accounts of Chemical Research 32, May 1999.
[2] R. Wiesendanger, Scanning Probe Microscopy and Spectroscopy: Methods and Applications, Cambridge University Press, Cambridge, 1994.
[3] S.N. Magonov, M.-H. Whangbo, Surface Analysis with STM and AFM, VCH, Weinheim, 1996.
[4] A. Noy, CD. Frisbie, L.F. Rozsnyai, M.S. Wrighton, CM. Lieber, J. Am. Chem. Soc. 117 (1995) 7943.
[5] E.L. Florin, V.T. Moy, H.E. Gaub, Science 264 (1994) 415.
[6] V.T. Moy, E.L. Florin, H.E. Gaub, Science 266 (1994) 257.
[7] Q. Zong, D. Innis, K. Kjoller, V.B. Elings, Surf. Sci. Lett. 290 (1993) L688.
[8] B.R.M. Gallot, Adv. Polym. Sci. 29 (1978) 85.
[9] B.R.M. Gallot, in: A. Blumstein (Ed.), Liquid Crystalline Order in Polymers, New York, Academic, 1978, p. 223.
[10] G. Riess, P. Bahadur, in: H.F. Mark, N.M. Bikales, C.G. Overberger, G. Menges (Eds.), Encyclopedia of Polymer Science and Engineering, Wiley, New York, 1989, p. 324.
[11] T. Hashimoto, K. Nagatoshi, A. Todo, H. Hasegawa, H. Kawai, Macromolecules 7 (1974) 364.
[12] T. Hashimoto, A. Todo, H. Itoi, H. Kawai, Macromolecules 10 (1977) 377.
[13] A. Todo, H. Kiuno, K. Miyoshi, T. Hashimoto, H. Kawai, Polym. Eng. Sci. 17 (1977) 587.
[14] T. Hashimoto, M. Shibayama, H. Kawai, Macro-molecules 13 (1980) 1237.
[15] T. Hashimoto, M. Fujimura, H. Kawai, Macromolecules 13 (1980) 1660.
[16] P.F. Green, T.M. Christensen, T.P. Russell, R. Jérôme, Macromolecules 22 (1989) 4600.
[17] P.F. Green, T.M. Christensen, T.P. Russell, Macromolecules 24 (1991) 252.
[18] G. Coulon, B. Collin, D. Ausserre, D. Chatenay, T.P. Russell, J. Phys. France 51 (1990) 2801.
[19] B. Collin, D. Chatenay, G. Coulon, D. Ausserre, Y. Gallot, Macromolecules 25 (1992) 1621.
[20] Ph. Leclĕre, R. Lazzaroni, J.L. Brédas, J.M. Yu, Ph. Dubois, R. Jérôme, Langmuir 12 (1996) 4317.
[21] G. Moineau, M. Minet, Ph. Dubois, Ph. Teyssié, T. Senninger, R. Jérôme (submitted for publication).
[22] G. Moineau, M. Minet, R. Jérôme (submitted for publication).
[23] J.D. Tong, Ph. Leclere, A. Rasmont, J.L. Bredas, R. Lazzaroni, R. Jerome (submitted for publication).
[24] Y.S. Yu, Ph. Dubois, R. Jérôme, P.h. Teyssié, Macromolecules 29 (1996) 1753.
[25] Y.S. Yu, Ph. Dubois, R. Jérôme, Ph. Teyssié, J. Polym. Sci. Part A: Polym. Chem. 34 (1996) 2221.
[26] L.M. Yu, Ph. Dubois, Ph. Teyssié, R. Jérôme, S. Blacher, F. Brouers, G. L'Homme, Macromolecules 29 (1996) 5384.
[27] J.M. Yu, Ph. Dubois, Ph. Teyssié, R. Jérôme, Macromolecules 29 (1996) 6090.
[28] J.M. Yu, Ph. Dubois, R. Jérôme, Macromolecules 29 (1996) 8362.
[29] J.M. Yu, R. Jérôme, Macromolecules 29 (1996) 8371.
[30] J.M. Yu, R. Jérôme, Ph. Teyssié, Polymer 38 (1997) 347.
[31] J.M. Yu, Y.S. Yu, Ph. Dubois, Ph. Teyssié, R. Jérôme, Polymer 38 (1997) 3091.
[32] L.M. Yu, S. Blacher, F. Brouers, G. L'Homme, R. Jérôme, Macromolecules 30 (1997) 4619.
[33] F.S. Bates, G.H. Fredrickson, in: G. Holden, N.R. Legge, R. Quirk, H.E. Schroeder (Eds.), Thermoplastic Elastomers, 2nd ed., Munich, Hanser, 1996, p. 335.
[34] G. Bar, Y. Thomman, R. Brandsch, H.J. Cantow, M.H. Whangbo, Langmuir 13 (1997) 3807.
[35] N.A. Burnham, O.P. Behrend, F. Oulevey, G. Gremaud, P.J. Gallot, D. Gourdon, E. Dupas, A.L. Kulik, H.M. Pollock, G.A.D. Briggs, Nanotechnology 8 (1997) 67.
[36] J.P. Cleveland, B. Anczykowski, A.E. Schmid, V.B. Elings, Appl. Phys. Lett. 72 (1998) 2613.
[37] S.N. Magonov, V. Elings, M.H. Whangbo, Surf. Sci. 375 (1997) L385.
[38] B. Anczykowski, J.P. Cleveland, D. Krüger, V. Elings, H. Fuchs, Appl. Phys. A 66 (1998) S885.
[39] J.P. Aimé, G. Couturier, R. Boisgard, L. Nony, Appl. Surf. Sci. 140 (1999) 333.
[40] R. Boisgard, D. Michel, J.P. Aimé, Surf. Sci. 401 (1998) 199.

[41] J.P. Aimé, D. Michel, R. Boisgard, L. Nony, Phys. Rev. B 59 (1999) 2407.
[42] L. Nony, R. Boisgard, J.P. Aimé, J. Chem. Phys. 111 (1999) (in press).
[43] S. Kopp-Marsaudon, Ph. Leclĕre, R. Lazzaroni, J.P. Aimé (in press).
[44] T.P. Russell, G. Coulon, V.R. Deline, D.C. Miller, Macromolecules 22 (1989) 2189.
[45] M.W. Matsen, M. Schick, Phys. Rev. Lett. 72 (1994) 2660.
[46] M.W. Matsen, M. Schick, Macromolecules 27 (1994) 6761.
[47] A.K. Khandpur, S. Förster, F.S. Bates, I.W. Hamley, A.J. Ryan, W. Bras, K. Almdal, K. Mortensen, Macromolecules 28 (1995) 8796.
[48] D.A. Hadjuk, P.E. Harper, S.M. Gruner, C. Honecker, G. Kim, E.L. Thomas, L.J. Fetters, Macromolecules 27 (1994) 4063.
[49] M.F. Schultz, F.S. Bates, K. Almdal, K. Mortensen, Phys. Rev. Lett. 73 (1994) 86.
[50] A. Avgeropoulos, B.J. Dair, N. Hadjichristidis, E.L. Thomas, Macromolecules 30 (1997) 5434.
[51] F.W. Billmeyer, Textbook of Polymer Science, 3rd ed., Wiley, New York, 1984.
[52] D.W. Van Krevelen, Properties of Polymers, 3rd ed., Elsevier, Amsterdam, 1990, p. 790.
[53] M.A. Van Dijk, R. Van den Berg, Macromolecules 28 (1995) 6773.
[54] G.C.L. Wong, J. Commandeur, H. Fisher, W.H. de Jeu, Phys. Rev. Lett. 77 (1996) 5221.
[55] S.H. Anastasiadis, T.P. Russell, S.K. Satija, C.F. Ma-jkrzak, Phys. Rev. Lett. 62 (1989) 1852.
[56] B.L. Carvalho, E.L. Thomas, Phys. Rev. Lett. 73 (1994) 3321.
[57] T.P. Russell, G. Coulon, V.R. Define, D.C. Miller, Macromolecules 22 (1989) 2189.
[58] G.J. Kellogg, D.G. Walton, A.M. Mayes, P. Lambooy, T.P. Russell, P.D. Gallagher, S.K. Satija, Phys. Rev. Lett. 76 (1996) 2503.
[59] T.L. Morkved, H.M. Jaeger, Europhys. Lett. 40 (1997) 643.